THE JOURNAL OF PHYSICAL CHEMISTRY B
A JOURNAL OF THE AMERICAN CHEMICAL SOCIETY

pubs.acs.org/JPCB

Article

Uncovering Differences in Hydration Free Energies and Structures for Model Compound Mimics of Charged Side Chains of Amino Acids

Published as part of The Journal of Physical Chemistry virtual special issue "Dave Thirumalai Festschrift".

Martin J. Fossat,[†] Xiangze Zeng,[†] and Rohit V. Pappu*

Cite This: *J. Phys. Chem. B* 2021, 125, 4148–4161

Read Online

ACCESS | Metrics & More | Article Recommendations

ABSTRACT: Free energies of hydration are of fundamental interest for modeling and understanding conformational and phase equilibria of macromolecular solutes in aqueous phases. Of particular relevance to systems such as intrinsically disordered proteins are the free energies of hydration and hydration structures of model compounds that mimic charged side chains of Arg, Lys, Asp, and Glu. Here, we deploy a Thermodynamic Cycle-based Proton Dissociation (TCPD) approach in conjunction with data from direct measurements to obtain estimates for the free energies of hydration for model compounds that mimic the side chains of Arg^+, Lys^+, Asp^-, and Glu^-. Irrespective of the choice made for the hydration free energy of the proton, the TCPD approach reveals clear trends regarding the free energies of hydration for Arg^+, Lys^+, Asp^-, and Glu^-. These trends include asymmetries between the hydration free energies of acidic (Asp^- and Glu^-) and basic (Arg^+ and Lys^+) residues. Further, the TCPD analysis, which relies on a combination of experimental data, shows that the free energy of hydration of Arg^+ is less favorable than that of Lys^+. We sought a physical explanation for the TCPD-derived trends in free energies of hydration. To this end, we performed temperature-dependent calculations of free energies of hydration and analyzed hydration structures from simulations that use the polarizable Atomic Multipole Optimized Energetics for Biomolecular Applications (AMOEBA) force field and water model. At 298 K, the AMOEBA model generates estimates of free energies of hydration that are consistent with TCPD values with a free energy of hydration for the proton of ca. −259 kcal/mol. Analysis of temperature-dependent simulations leads to a structural explanation for the observed differences in free energies of hydration of ionizable residues and reveals that the heat capacity of hydration is positive for Arg^+ and Lys^+ and negative for Asp^- and Glu^-.

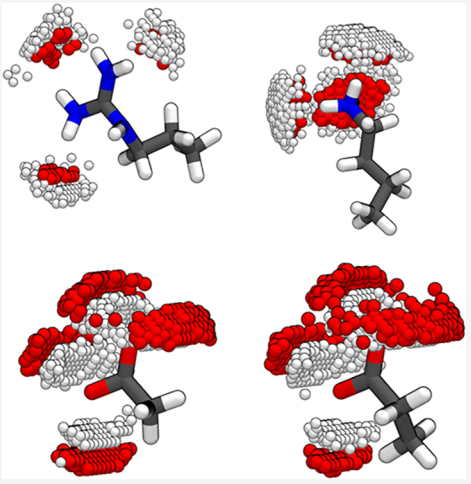

1. INTRODUCTION

There is growing interest in uncovering the sequence-specific conformational preferences of intrinsically disordered proteins (IDPs)[1] and in using these insights to quantify sequence-specific contributions to the driving forces for phase separation.[2] In a purely additive model,[3] sequence-ensemble relationships of IDPs can be rationalized using the free energies of hydration of model compound mimics of side-chain and backbone moieties.[4] Indeed, the molecular transfer model of Thirumalai and co-workers[5] is a direct illustration of how free energies of solvation can be used to obtain predictive, coarse-grained descriptions of conformational transitions of proteins as a function of changes to solution conditions.[6]

At a specific temperature and pressure, the free energy of hydration ($\Delta\mu_h$) is defined as the change in free energy associated with transferring the solute of interest from a dilute vapor phase into water.[7] Vapor pressure osmometry was an early method adopted by Wolfenden[8] to measure free energies of hydration. While this works for polar solutes, including neutral forms of ionizable species, it cannot be used to measure free energies of hydration of ionizable residues because of the ultralow vapor pressures and the confounding effects of ion pairing in the gas phase. Calorimetry[9] is also problematic because of the large magnitudes of free energies of hydration for ionizable residues.[10] And because stable solutions are electro-neutral,[10b] estimates of free energies of hydration of ionic species have to rely on parsing numbers derived from measurements of

Received: February 5, 2021
Revised: April 7, 2021
Published: April 20, 2021

https://doi.org/10.1021/acs.jpcb.1c01073
J. Phys. Chem. B 2021, 125, 4148–4161

whole salts against those of a suitable reference system.[11] Parsing measurements for whole salts also rests on the assumption of minimal ion pairing or clustering, which need not be true in general, especially for organic ions.[12]

Here, we incorporate updated estimates for a series of experimentally measured quantities and combine these with a **T**hermodynamic **C**ycle based on **P**roton **D**issociation (TCPD)—see Figure 1—to obtain a distribution of experimentally derived estimates for free energies of hydration of charged amino acids at 298 K.[13] This approach uses inputs from (i) direct measurements of proton dissociation energies in the gas phase; (ii) measured pK_a values in the aqueous phase—including recent updates based on revisited measurements for the pK_a of Arg;[14] (iii) measured free energies of hydration of uncharged variants of charged residues; and (iv) a collection of 72 different computed and experimentally derived estimates of $\Delta\mu_h^{H^+}$, the proton free energy of hydration at 298 K.

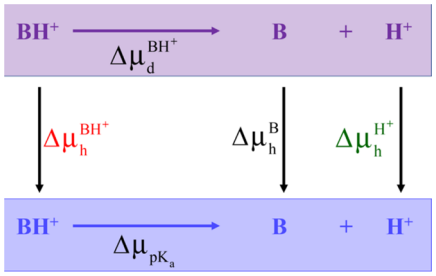

Figure 1. Illustration of the TCPD approach. The schematic shows the transfer of a strong base and the proton dissociation reaction from the gas phase (purple) into the aqueous phase (blue).

The TCPD approach is motivated by the separate albeit complementary efforts of Sitkoff et al.,[15] Pliego and Riveros,[16] and Zhang et al.[17] We follow closely the approach of Pliego and Riveros, who estimated absolute values for $\Delta\mu_h$ for 30 different univalent ions, many of which are organic ions. They relied on the estimates for the free energy of hydration of the proton provided by Tissandier et al.[18] There were challenges with obtaining $\Delta\mu_h$ for the model compound that mimics the Arg^+ side chain because of persistent uncertainties regarding its pK_a[14] in the aqueous phase and the absence of data for proton dissociation in the gas phase. Improved estimates are now available for all the relevant quantities. We adapted these for obtaining TCPD-derived values for the free energies of hydration of charged amino acids as illustrated in Figure 1. The TCPD-derived estimates serve as updated reference values for the free energies of hydration of charged amino acids, which will depend on the choice one makes for $\Delta\mu_h^{H^+}$. We show that free energies calculated using the polarizable Atomic Multipole Optimized Energetics for Biomolecular Applications (AMOEBA) force field for water and model compound mimics of the side chains of Arg^+, Lys^+, Asp^-, and Glu^- reproduce the trends obtained using the TCPD analysis. The simulations were then analyzed to obtain comparative assessments of hydration structures. This yields a physical picture for the trends we observe for free energies of hydration of model compounds that mimic side chains of charged residues.

2. METHODS

2.1. Details of the TCPD Approach. Concepts underlying the TCPD approach are summarized in Figure 1. The model compounds used as mimics for the ionized versions of the side chains are 1-propylguanidinium (Arg^+), 1-butylammonium (Lys^+), acetate (Asp^-), and propionate (Glu^-). For bases, deprotonation reactions in the gas and aqueous phases are written as $BH^+ \overset{\Delta\mu_d^{BH^+}}{\rightleftharpoons} B + H^+$ and $BH^+ \overset{\Delta\mu_{pK_a}}{\rightleftharpoons} B + H^+$, respectively. Here, $\Delta\mu_d^{BH^+}$ quantifies the change in free energy that accompanies the dissociation of a proton from the base in the gas phase,[19] whereas $\Delta\mu_{pK_a}$ is the equivalent quantity in the aqueous phase.[20] The free energy of proton dissociation in the aqueous phase can be obtained from knowledge of the pK_a for the model compound of interest whereby $\Delta\mu_{pK_a} = RT\ln(10^{pK_a})$. Here, $R = 1.987\,17 \times 10^{-3}$ kcal/(mol K), and T is set to 298 K. This approach is the complement of the method used by Jorgensen and Briggs.[21] The use of measured values of $\Delta\mu_d^{BH^+}$ and $\Delta\mu_h^{B}$ combined with an estimation of $\Delta\mu_{pK_a}$, based on measured pK_a values, and knowledge of the free energy of hydration of the proton $\Delta\mu_h^{H^+}$ allows the usage of a TCPD analysis to obtain the free energy of hydration $\Delta\mu_h^{BH^+}$ of the protonated base as shown in Equation 1.

$$\Delta\mu_h^{BH^+} = (\Delta\mu_h^{B} + \Delta\mu_d^{BH^+} - \Delta\mu_{pK_a} + \Delta\mu_h^{H^+}) \quad (1)$$

Likewise, for acids, the free energies of hydration ($\Delta\mu_h^{A^-}$) of the deprotonated forms are calculated using Equation 2.

$$\Delta\mu_h^{A^-} = (\Delta\mu_h^{AH} - \Delta\mu_d^{AH} + \Delta\mu_{pK_a} - \Delta\mu_h^{H^+}) \quad (2)$$

Here, $\Delta\mu_d^{AH}$ is the free energy of hydration of the protonated form of the acid, which is measured directly,[22] and $\Delta\mu_d^{AH}$ quantifies the change in free energy that accompanies the dissociation of a proton from the acid in the gas phase; the value to be used for $\Delta\mu_h^{H^+}$ is identical to that of Equation 1. In Equations 1 and (2), $\Delta\mu_{pK_a} = 2.30\,(RT)(pK_a)$ is estimated using measured pK_a values of the base[23] or acid, respectively.

The TCPD approach has been proposed[24] and used in the literature,[16] and its usage requires accurate measurements of the relevant parameters.[17] These are now available in the form of accurate proton dissociation/association energies in the gas phase, well-established and reliable values for $\Delta\mu_h^{B}$ and $\Delta\mu_h^{AH}$, and improved estimates of the pK_a values, specifically for the Arg^+ side chain. As for $\Delta\mu_h^{H^+}$, we found 72 distinct estimates (Table 1) in the literature. The mean value is -260.89 ± 5.82 kcal/mol. In this work, we obtain TCPD estimates for the free energies of hydration of Arg^+, Lys^+, Asp^-, and Glu^- as a function of 72 distinct estimates for the free energy of hydration of the proton.

2.2. Setup of Simulations using the AMOEBA Force Field. The free energy calculations we report here are an extension of the recent simulations performed by Zeng et al.[4] The authors developed parameters of the requisite model compounds for the AMOEBA force field. The details of the force field parametrization, the setup of the simulations, and free energy calculations may be found in the work of Zeng et al.[4] In the interest of completeness, we include a summary of the overall simulation setup and an analysis of simulation results.

Simulations were performed using the TINKER-OpenMM package.[50] For each model compound, the simulations were performed using a cubic water box with periodic boundary conditions. The initial dimensions of the central cell were set to

https://doi.org/10.1021/acs.jpcb.1c01073
J. Phys. Chem. B 2021, 125, 4148−4161

Table 1. 72 Distinct Values for the Proton Free Energy of Hydration Collated from the Literature[a]

$\Delta\mu_h^{H^+}$ (kcal/mol)	reference	methods
−247.00	Lamoureux et al.[25]	Molecular dynamics simulations with a polarizable forcefield based on the Drude model
−251.43	Schmid et al.[26]	Hydration entropy is obtained based on the thermodynamics of the dissociation of water. Hydration enthalpy is obtained based on the relation between hydration entropy and hydration enthalpy proposed by Krestov.[27]
−252.39, −253.08, −253.18, −253.27, −253.30, −253.49, −253.54, −253.66, −254.90, −255.23	Marković et al.[28]	Quantum mechanical (QM) calculations with the solvation model based on density (SMD)
−258.26	Grossfield et al.[11] and this work	The intrinsic free energy of hydration was estimated by Grossfield et al., using the known free energy difference between K^+ and H^+ and AMOEBA derived intrinsic free energies of hydration for K^+. The value reported by Grossfield et al., was −252.5 kcal/mol for the intrinsic free energy of hydration. Beck has estimated the Galvani potential for the AMOEBA water model to be −0.25 V, which corresponds to a correction of −5.76 kcal/mol, leading to the final estimate of −258.26 kcal/mol for the corrected free energy of hydration of the proton for the AMOEBA model.
−254.60	Asthagiri et al.[29]	Quasi-chemical theory
−253.40	Latimer et al.[30]	The Born equation with additional assumptions is used to calculate the free energy of cations and ions.
−253.40	Carvalho and Pliego[31]	Cluster continuum quasi-chemical theory
−254.28	Marcus[32]	A correction term for the compression of the space available to the ion on its transfer from its gaseous to its aqueous standard states is made to the value −252.39 kcal/mol (−1056 kJ/mol)
−256.93	Duignan et al.[33]	Estimates are made using the established difference in the free energy of hydration between Li^+ and H^+. The free energy of hydration of Li^+ is calculated using DFT interaction potentials with molecular dynamics simulations (DFT-MD) combined with a modified version of the quasi-chemical theory.
−259.50	**Pearson**[13]	**Based on the absolute potential of hydrogen electrode**
−260.28	Vlcek et al.[34]	A correction for the surface potential is made to the value from cluster pair approximation.
−260.50	**Friedman and Krishnan**[35]	**Parsing of data using a reference salt tetraphenyl arsonium tetraphenyl borate (TATB) method**
−260.76	**Fawcett**[36]	**Fit to data from measurements of the ionic work function**
−258.80	Yu et al.[37]	Simulations based on a forcefield that uses the Drude model for atomic polarizabilities
−262.40	Zhan and Dixon[38]	QM calculations for the ion−water cluster and a self-consistent reaction field model for the interaction between the cluster and solvent
−262.38, −261.86	Hofer and Hünenberger[39]	QM/MM simulations and thermodynamic integration
−261.73, −262.23, −262.27, −262.67,	Tawa et al.[40]	QM calculations for the ion−water cluster and a self-consistent reaction field model for the interaction between the cluster and solvent
−261.86, −262.38, −262.89	Prasetyo et al.[41]	QM/MM simulations and thermodynamics integration
−262.91	Reif and Hünenberger[42]	Inferred from hydration structures obtained using classical molecular dynamics simulations
−263.79	Tuttle et al.[43]	Cluster pair approximation method
−263.98	Tissandier et al.[18]	Cluster pair approximation method
−264.20	Pollard and Beck[44]	Quasi-chemical theory analysis of cluster pair approximation
−256.75, −254.26, −259.75, −262.46, −254.75, −261.50, −252.05, −268.35, −265.22, −265.15, −267.54, −267.30, −266.67, −265.17, −266.04, −265.43, −265.46	Matsui et al.[45]	Based on the relationship between pK_a value, free energy of solvation of the neutral and charged versions of small molecules and free energy of solvation of proton. Experimental pK_a values are used. Free energy of solvation of the neutral and charged versions of small molecules are calculated from QM with continuum solvent model.
−266.10, −268.40, −266.60, −265.10, −267.80, −265.80, −264.40, −271.30, −267.70, −263.70, −269.30, −266.80, −266.10, −268.00	Kelly et al.[46]	Cluster pair approximation method
−266.40	Rossini and Knapp[47]	Uses quantum chemical density functional theory calculations of proton affinity in the gas phase and use of the Poisson equation to compute solvation contributions.
−252.50, −266.70	Bryantsev et al.[48]	Cluster Continuum Model

https://doi.org/10.1021/acs.jpcb.1c01073
J. Phys. Chem. B 2021, 125, 4148−4161

Table 1. continued

$\Delta\mu_h^{H^+}$ (kcal/mol)	reference	methods
−267.88	Ishikawa and Nakai[49]	Cluster Continuum Model

[a]Rows that are bold-faced are estimates from an analysis of experimental data without the use of any simulations. This is noteworthy because the mean value of −260.89 is closest to estimates derived from parsing of experimental data, sans any calculations.

be 30 × 30 × 30 Å^3. All molecular dynamics simulations were performed using the RESPA integrator[51] with an inner time step of 0.25 ps and an outer time step of 2.0 fs in isothermal−isobaric ensemble (NPT) ensemble. The target temperature was set to be one of 275, 298, 323, 348, or 373 K, and the target pressure was set to be 1 bar. The temperature and pressure were controlled using a stochastic velocity rescaling thermostat[52] and a Monte Carlo constant pressure algorithm,[53] respectively. The particle mesh Ewald (PME) method,[54] with PME-GRID being 36 × 36 × 36, and *B*-spline interpolation,[55] with a real space cutoff of 7 Å, was used to compute long-range corrections to electrostatic interactions. The cutoff for van der Waals interactions was set to be 12 Å. This combination has been verified[56] in previous work for AMOEBA-based free energy simulations.[57]

2.3. Free Energy Calculations. We used the Bennett Acceptance Ratio (BAR)[58] and Multistate Bennett Acceptance Ratio (MBAR)[59] methods to estimate the intrinsic free energies of hydration ($\Delta\mu_{h,intrinsic}$) for the model compounds of interest. Details of the simulation setup are identical to those of Zeng et al.[4] The solute is grown in using two different Kirkwood coupling parameters λ_{vdW} and λ_{el} that scale the strengths of solute−solute and solute−solvent van der Waals and electrostatic interactions. A series of independent molecular dynamics simulations were performed in the NPT ensemble for different combinations of λ_{vdW} and λ_{el}. A soft-core modification of the Buffered-14−7 function was used to scale the van der Waals interactions as implemented in Tinker-OpenMM.[50] For each pair of λ values, we performed simulations, each of length 6 ns, at the desired temperature and a pressure of 1 bar. We then used the TINKER bar program and the pymbar package https://github.com/choderalab/pymbar to calculate the free energy difference between neighboring windows defined in terms of the scaling coefficients. For every combination of λ_{vdW} and λ_{el}, we set aside the first 1 ns simulation as part of the equilibration process. In Appendix A, we show results from our analysis of the BAR-derived free energy estimates for different λ schedules.

2.4. From Intrinsic Free Energies of Hydration to Corrected Values. Following the rigorous definitions of free energies of hydration,[7] it follows that the transfer of an ionic solute from a fixed position in the gas phase (vacuum) to a fixed position in the water sets up a contribution from the crossing of the interface between the gas and aqueous phases.[60] This interface cannot be captured in simulations that use periodic boundary conditions.[61] Accordingly, the free energies of hydration that we obtain using protocols described in Sections 2.2 and 2.3 are intrinsic free energies. These have to be corrected by the contributions of the surface potential, known as the Galvani potential and denoted as Φ_G. The corrected free energy of hydration is calculated using the relation[62]

$$\Delta\mu_{h,corrected} = \Delta\mu_{h,intrinsic} + q\Phi_G$$

Beck has estimated the Galvani potential for the AMOEBA water model to be −0.25 V/*e*.[63] This translates to −5.76 kcal/mol/*e*. Accordingly, the corrected free energies of hydration, for the AMOEBA force field, are estimated using the intrinsic free energies of hydration calculated as described in Section 2.3, Beck's estimate for the Galvani potential, and setting q to +1 for Arg^+ and Lys^+ and q to −1 for Asp^- and Glu^-.

3. RESULTS

3.1. Free Energies of Hydration Calculated using the TCPD Approach. Values of free energies of hydration for

https://doi.org/10.1021/acs.jpcb.1c01073
J. Phys. Chem. B 2021, 125, 4148−4161

model compound mimics of Arg^+, Lys^+, Asp^-, and Glu^- side chains were calculated at 298 K using the TCPD approach—see Equations 1 and (2) and Figure 1. The difference between the gas-phase basicity[64] and $\Delta\mu_h^{H^+}$ quantifies the relative importance of bond energy and the free energy of solvation. Positive values for this difference imply that the favorable free energy of hydration of the proton cannot compensate for the loss of bond energy in the gas phase. In order to achieve the target pK_a value for the ionizable moiety, suitably large magnitudes for $\Delta\mu_h^{BH^+}$ and $\Delta\mu_h^{A^-}$ help offset the loss of bond energy in the gas phase. Values of $\Delta\mu_{pK_a}$ are derived from measurements of pK_a values for the relevant model compound mimics of Arg^+, Lys^+, Asp^-, and Glu^-. The pK_a values of all four model compounds were taken from the Physical/Chemical Property Database (PHYSPROP)[3] database, and they reflect updates from the measurements of Fitch et al.[14] and Xu et al.[65] These measurements move the consensus estimate for the pK_a of Arg up from 12.6 and 13.2[15] to 13.6. Values for free energies of hydration for uncharged constructs, that is, $\Delta\mu_h^B$ and $\Delta\mu_h^{AH}$, were obtained from the Hydration Free Energy Database curated by Mobley and Guthrie.[7]

The gas-phase dissociation energies $\Delta\mu_d^{BH^+}$ and $\Delta\mu_d^{AH}$, estimated from gas-phase basicity measurements,[64] are available from the literature for three of the four model compounds. Gas-phase basicity measurements of side-chain mimicking model compounds were taken from the National Institute of Standards and Technology (NIST) for acetic acid, propanoic acid, and 1-butylammonium. Experimental data for 1-propylguanidine are unavailable. Instead, we used results from gas-phase quantum-mechanical calculations for 1-methylguanidine.[64] These calculations yield excellent agreement for gas-phase basicities as compared to experimental values obtained for a range of model compounds. The differences in electronic structure between 1-propylguanidine and 1-methylguanidine are considerably smaller than the differences in electronic structures of 1-methylguanidine and guanidine. Accordingly, we use the calculated gas-phase basicity value for 1-methylguanidine as a more suitable proxy for the basicity of 1-propylguanidine. This is relevant because, in their deployment of the TCPD approach, Zhang et al.[17] used guanidine as a model compound to mimic the Arg side chain. The difference in gas-phase basicities of 1-methylguanidine and guanidine is greater than 7 kcal/mol. Accordingly, the use of basicity values for guanidine results in a significant overestimation of the magnitude of the of $\Delta\mu_h$ for the Arg^+ side chain.

The free energy of hydration of the proton $\Delta\mu_h^{H^+}$ is a crucial parameter that determines the outputs we obtain from the TCPD approach. We combed the literature and found at least 72 distinct estimates for $\Delta\mu_h^{H^+}$—see Table 1 and Figure 2. As summarized in Table 1, the approaches used to obtain estimates of $\Delta\mu_h^{H^+}$ combine quantum-mechanical calculations, empirical considerations/prescriptions, and bespoke interpretations of experimental data for whole salts or pK_a values. The distribution of tabulated values yields a mean of -260.89 ± 5.82 kcal/mol for $\Delta\mu_h^{H^+}$ at 298 K. Instead of choosing a specific value for $\Delta\mu_h^{H^+}$, we compute the values of the free energies of hydration ($\Delta\mu_h$) for Arg^+, Lys^+, Asp^-, and Glu^- for each of the 72 tabulated values of$\Delta\mu_h^{H^+}$. The values we obtain for $\Delta\mu_h$ are plotted as a function of values used for $\Delta\mu_h^{H^+}$ (Figure 3).

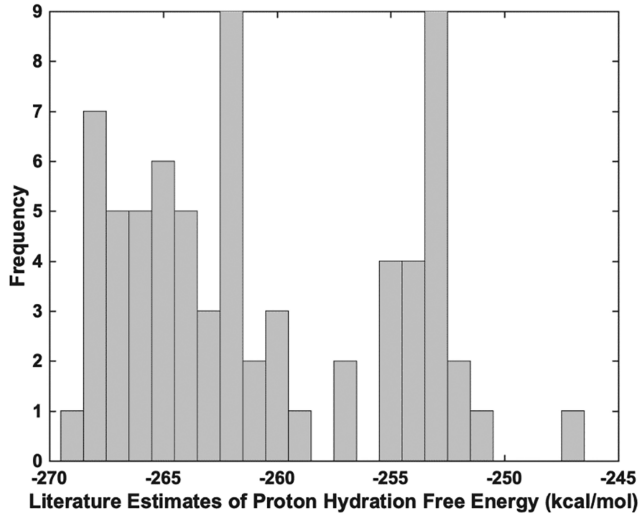

Figure 2. Distribution of tabulated values for the proton hydration free energy at 298 K. These values are listed in Table 1 and were collated from the literature.

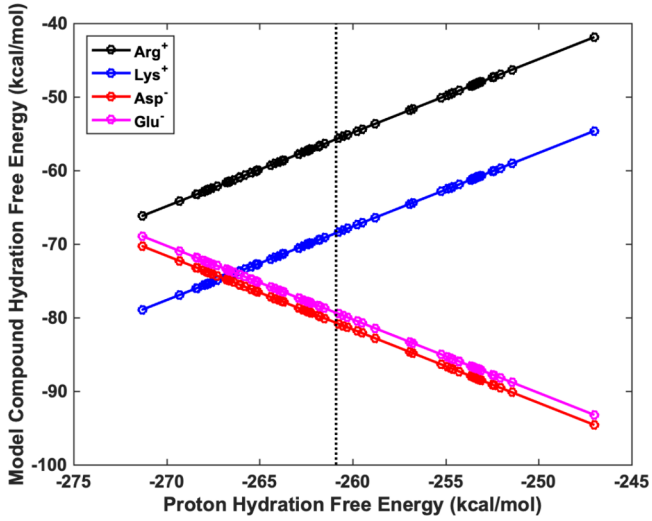

Figure 3. TCPD-derived free energies of hydration at 298 K. The data are plotted against the literature-derived proton hydration free energies (circles). The solid lines join the circles and are included as guides. The vertical dotted line intersects the abscissa at the mean value of −260.89 kcal/mol for the proton hydration free energy.

Results from the application of the TCPD approach are summarized in Table 2. In addition to the values of $\Delta\mu_h^{BH^+}$ and $\Delta\mu_h^{A^-}$ obtained using the mean value of $\Delta\mu_h^{H^+}$ from Table 1, we also tabulate the values used for measured and/or calculated gas-phase basicity values, measured pK_a values, and free energies of hydration for the uncharged forms of the model compounds. These estimates are for a temperature of 298 K. As expected, the estimated free energies of hydration are large and negative. However, the TCPD-based estimates revealed unexpected trends. Despite being a strong base, the estimated value of $\Delta\mu_h$ is ∼12 kcal/mol less favorable for Arg^+ when compared to Lys^+. Further, the estimates for $\Delta\mu_h$ of Arg^+ and Lys^+ are smaller in magnitude than those for Asp^- and Glu^-. The acids are more favorably hydrated than bases—an observation that is concordant with results for free energies of hydration of small anions versus cations.[66]

https://doi.org/10.1021/acs.jpcb.1c01073
J. Phys. Chem. B 2021, 125, 4148−4161

Table 2. Summary of Inputs to and Outputs from the TCPD Approach Used for Estimating Values of Free Energies of Hydration for Arg^+, Lys^+, Asp^-, and Glu^-

side chain mimicked by the model compound	measured[67] pK_a	gas-phase basicity (kcal/mol)[19,68]	measured values of $\Delta\mu_h^B$,$\Delta\mu_h^{AH}$ (kcal/mol)[64]	$\Delta\mu_h^{BH^+}$,$\Delta\mu_h^{A^-}$ derived from TCPD analysis using the mean value[a] for $\Delta\mu_h^{H^+}$ (kcal/mol)[c]
Arg^+	13.6[65]	234.6 ± 2.0[b]	−10.9 ± 1.9	−55.76 ± 6.44
Lys^+	10.7[69]	211.3 ± 0.5	−4.3 ± 1.9	−68.51 ± 6.15
Asp^-	4.76[70]	341.4 ± 1.2	−6.7 ± 1.9	−80.71 ± 6.24
Glu^-	4.88[70]	340.4 ± 1.4	−6.5 ± 1.9	−79.35 ± 6.28

[a]The mean and standard deviation of $\Delta\mu_h^{H^+}$ calculated from the literature values (Table 1) are −260.89 ± 5.82 kcal/mol. Irrespective of the value used for the free energy of hydration of the proton, the free energy of hydration of the model compound mimic of Arg^+ is 12.75 kcal/mol less favorable than that of Lys^+. Conversely, the free energies of hydration of model compound mimics of Asp^- and Glu^- are ∼25 and ∼24 kcal/mol more favorable than that of Arg^+ and ∼12 and ∼11 kcal/mol more favorable than that of Lys^+ when we set $\Delta\mu_h^{H^+}$ = −260. 89 kcal/mol. [b]This is the calculated gas-phase basicity for 1-methylguanidinium. Note that the value of the gas-phase basicity for guanidinium is 226.9 kcal/mol. The value we use is more appropriate for 1-propylguanidinium. [c]The large error bars in this column are entirely due to the large standard deviation of 5.82 kcal/mol that we compute across the 72 distinct values we collated for the hydration free energy of the proton.

Table 3. Summary of Results Obtained from Calculations of Intrinsic Free Energies of Hydration ($\Delta\mu_{h,intrinsic}$) Derived from Free Energy Calculations using the AMOEBA Force Field

side chain mimicked by the model compound	$\Delta\mu_{h,intrinsic}$ (kcal/mol) 275 K	$\Delta\mu_{h,intrinsic}$ (kcal/mol) 298 K	$\Delta\mu_{h,intrinsic}$ (kcal/mol) 323 K	$\Delta\mu_{h,intrinsic}$ (kcal/mol) 348 K
Arg^+	−47.63 ± 0.11	−46.72 ± 0.11	−45.67 ± 0.11	−45.45 ± 0.09
Lys^+	−61.22 ± 0.10	−60.49 ± 0.09	−59.53 ± 0.09	−58.99 ± 0.08
Asp^-	−90.39 ± 0.08	−89.91 ± 0.08	−89.02 ± 0.07	−88.15 ± 0.07
Glu^-	−86.84 ± 0.12	−86.16 ± 0.12	−85.24 ± 0.12	−84.32 ± 0.11

3.2. Prescription for Comparing Computed Free Energies of Hydration to TSPD Estimates. The large and persistent uncertainties in estimates of the free energy of hydration of the proton make it impossible to obtain precise, experimentally derived values of $\Delta\mu_h$ for Arg^+, Lys^+, Asp^-, and Glu^-. However, one can prescribe a measure of consistency that can be used to judge the accuracy of a force field calculation. If we denote the force field and water model specific proton free energy as $\Delta\mu_{h,FF}^{H^+}$, then the force field derived estimates of $\Delta\mu_h$ for Arg^+, Lys^+, Asp^-, and Glu^- would have to be similar to the TCPD-derived estimate obtained by setting $\Delta\mu_h^{H^+} = \Delta\mu_{h,FF}^{H^+}$. This level of consistency is the best one can hope for pending the availability of a data-driven consensus regarding the precise value for $\Delta\mu_h^{H^+}$. The approach we propose for assessing consistency with the TCPD approach guards against imposing false standards based on definitive assertions that in reality will always depend on the choice one makes for $\Delta\mu_h^{H^+}$.

3.3. Free Energy Calculations Based on the AMOEBA Force Field Yield Values That Are Consistent with a Proton Free Energy of Hydration of −258.26 kcal/mol. For each of the model compounds, we used the AMOEBA force field and water model[71] used to calculate intrinsic free energies of hydration at four different temperatures, specifically, 275, 298, 323, and 348 K. The results are summarized in Table 3.

When estimates for the Galvani potential in the AMOEBA water model[63] and the intrinsic proton free energy of hydration reported by Grossfield et al. are combined,[11] the corrected value for the free energy of hydration of the proton at 298 K is −258.26 kcal/mol for the AMOEBA force field. We calculate the root-mean-squared deviation (RMSD) to be 0.97 kcal/mol between the corrected free energies of hydration calculated using the AMOEBA force field and those estimated using the TCPD approach by setting $\Delta\mu_h^{H^+}$ = −258.26 kcal/mol (Table 4). The RMSD being within a kilocalorie per mole suggests that the free energies of hydration we obtain for Arg^+, Lys^+, Asp^-, and Glu^- are consistent with experimental data for the experimentally derived TCPD-based estimates if we use the proton free energy of hydration that is consistent with that of the AMOEBA force field.

Table 4. Comparison of Corrected Free Energies of Hydration from AMOEBA at 298 K to TCPD Estimates Obtained using a Proton Free Energy of Hydration of −258.26 kcal/mol

side chain	corrected AMOEBA kcal/mol (I)	TCPD estimates kcal/mol (II)	residuals I−II kcal/mol
Arg^+	−53.39 ± 0.11	−53.13	−0.26
Lys	−66.98 ± 0.10	−65.88	+1.10
Asp	−84.63 ± 0.08	−83.34	+1.29
Glu	−81.08 ± 0.12	−81.98	−0.90

How do the corrected estimates for $\Delta\mu_h$ obtained using simulations based on the AMOEBA force field compare to estimates obtained using other instantiations of polarizable force fields? To answer this question, we compared our results to those reported by Lin et al., using the classical Drude oscillator model.[72] The molecular ions studied by Lin et al. include 1-methylguanidinium and acetate. Lin et al. report a value of −84.7 ± 0.1 kcal/mol for acetate. In comparison, the corrected value we obtain for acetate using the AMOEBA force field is −84.63 ± 0.08 kcal/mol. Further, as noted in Table 4, the value we obtain using the AMOEBA force field is within 1.29 kcal/mol of the value we derive from the TCPD approach, providing we set the hydration free energy of the proton to be −258.26 kcal/mol—the value for the AMOEBA force field. Lin et al. reported a value of −59.3 kcal/mol for 1-methylguanidinium. The value we obtain from AMOEBA simulations for 1-propylguanidinium is −53.39 kcal/mol. Although direct comparisons between the free energies of hydration for the model compounds are confounded by differences in the side-chain structure, Table 4 clearly shows that the TCPD-derived estimate, which uses the gas-phase basicity for 1-methylguanidinium, is closer to the AMOEBA-

https://doi.org/10.1021/acs.jpcb.1c01073
J. Phys. Chem. B 2021, 125, 4148−4161

derived value for 1-propylguanidinium. If we use the mean value of −260.89 for the free energy of hydration of the proton, we estimate the free energy of hydration for 1-propylguanidinium to be −55.76 kcal/mol as shown in Table 2. This is closer to the value we derive using simulations based on the AMOEBA force field when compared to the value reported by Lin et al. for 1-methylguanidinium.

3.4. Insights from Analysis of the Temperature Dependence of Calculated Free Energies of Hydration. Table 3 shows how the intrinsic free energies of hydration vary with temperature for each of the model compounds. The consistent trend is of the intrinsic free energies of hydration becoming less favorable as temperature increases. We fit the temperature-dependent data for the intrinsic free energies of hydration to the integral of the Gibbs−Helmholtz equation in order to estimate the intrinsic enthalpy of hydration (Δh) and intrinsic heat capacity of hydration (Δc_p) at a reference temperature of 298 K. In doing so, we assume that values of Δh and Δc_p are independent of temperature, a conjecture that is supported by the linear increase in the magnitudes of $\Delta\mu_h^{BH^+}$ and $\Delta\mu_h^{A^-}$ with increasing temperature. The integral of the Gibbs−Helmholtz equation is written as

$$\Delta\mu_{h,intrinsic}(T) = \frac{[\Delta\mu_{h,intrinsic}(T_0) - \Delta h]T}{T_0} + \Delta h + \Delta c_p\left[T\left(1 - \ln\frac{T}{T_0}\right) - T_0\right] \quad (3)$$

To use Equation 3, we set T_0 = 298 K, substitute the calculated value of $\Delta\mu_{h,intrinsic}(T_0)$, and estimate Δh and Δc_p using a Levenberg−Marquardt nonlinear least-squares algorithm. The values we obtain for Δh and Δc_p are shown in Table 5. As a test of the quality of the fit, we compare the values of $\Delta\mu_{h,intrinsic}(T)$ from free energy calculations to those obtained using Equation 3. For the latter, we use the parameters listed in Table 5. The comparisons are shown in Figure 4.

Table 5. Parameters for Δh and Δc_p Extracted from Nonlinear Least Squares Analysis of Computed Temperature-Dependent Free Energies and Fits to eq 3

side chain mimicked by the model compound	estimated Δh at 298 K (kcal/mol)	estimated Δc_p (cal/(mol K))
Arg^+	−57.24	69.39
Lys^+	−70.37	29.98
Asp^-	−98.65	−44.97
Glu^-	−96.62	−8.75

3.5. Analysis of Temperature-Dependent Intrinsic Values of Enthalpy and Entropy of Hydration. Using the Gibbs−Helmholtz equation and parameters shown in Table 5, we estimated the temperature dependence of the intrinsic enthalpy and entropy of hydration using Equation 4 below:

$$\Delta h(T) = \Delta h(T_0) + \Delta c_p(T - T_0)$$
$$\Delta s(T) = -\frac{[\Delta\mu_h(T_0) - \Delta h(T_0)]}{T_0} + \Delta c_p \ln\left(\frac{T}{T_0}\right) \quad (4)$$

The results are shown in Figure 5. There is a clear difference in the temperature dependencies for basic versus acidic molecules. With increasing temperature, the enthalpy of hydration becomes less favorable for Arg^+ and Lys^+, while it becomes more favorable for Asp^- and Glu^-. The unfavorable entropic contribution to the free energy of hydration stays roughly constant for Lys^+ and decreases with increasing temperature for Arg^+. In contrast, the unfavorable entropic contribution to the free energy of hydration increases with increasing temperature for Asp^- and Glu^-. Each of the results shown in Figure 5 is a direct consequence of the negative heat capacity of hydration for Asp^- and Glu^-, which contrasts with the positive heat capacity of hydration for Arg^+ and Lys^+ and all other model compounds that mimic backbone and side-chain moieties.

To understand the origins of the observations summarized in Figure 5, we performed three sets of reference simulations, one for the Cl^- ion and two for alchemic variants of the Cl^- ion. The anionic Cl^- ion is weakly polarizable in the AMOEBA model and carries a net charge of $-e$. We computed free energies of hydration for the following temperatures: 275, 298, 323, 348, and 373 K. The results for intrinsic free energies of hydration as a function of temperature are shown in Table 6. Here, we also show results for two alchemic versions of the Cl^- ion, namely, an uncharged version Cl^0 and a cationic version Cl^+, where we flip the sign of the charge. From the temperature-dependent values of the intrinsic free energies of hydration for Cl^-, Cl^0, and Cl^+ we extract estimates for the intrinsic enthalpy of hydration Δh at 298 K and the heat capacity of hydration Δc_p. These values are also tabulated in Table 6. A comparison of the parameters in Tables 5 and 6 reveals the following: Anions that mimic Asp^- and Glu^- and the Cl^- ion have negative Δc_p values. The magnitude of Δc_p decreases and approaches zero as the length of the alkyl chain increases—see comparisons of Δc_p values for mimics of Asp^- versus Glu^-. The Δc_p values are positive for model compound mimics of Arg^+, Lys^+, and the alchemic Cl^+ ion. The magnitude of the positive Δc_p increases with hydrophobicity, and surprisingly, 1-propylguanidinium has a higher Δc_p when compared to the neutral, alchemic Cl^0 solute. These numerical findings prompted detailed comparisons of hydration structures, and these are presented next.

3.6. Comparative Analysis of Hydration Structures around the Different Solutes. Molecular theories for hydrophobic and hydrophilic hydration rest on comparative analyses of hydration structures around solutes and the effects of solutes on density inhomogeneities within water. The chemical structures of the mimics of Arg^+, Lys^+, Asp^-, and Glu^- are subtly or significantly different from another. We computed the spatial density profiles of water molecules around each of the solutes. The results from this analysis are summarized pictorially in Figure 6. Here, each panel shows regions around each solute where the density of oxygen and hydrogen atoms from water molecules rises above a prescribed cutoff value—see caption. These calculations emphasize the accumulation of water molecules around the functional groups within each solute.

The distinction between hydrophobic and hydrophilic hydration is typically attributed to differences in the hydration structure within the first hydration shell,[74] to the spatial organization of the first shell with respect to the bulk,[74,75] to density inhomogeneities in the vicinity of the solute,[76] and their long-range effects.[77] We quantify hydration structures in terms of two-parameter probability distribution functions. Here, we follow the approach of Gallagher and Sharp[75] and compute the joint radial and angular distribution functions $\rho(r,\theta)$ where the definition of r and θ are as shown in Figure 7. For neat water, the distribution functions are computed using all pairs of water molecules that are within 8 Å of one another. For solute−solvent

https://doi.org/10.1021/acs.jpcb.1c01073
J. Phys. Chem. B 2021, 125, 4148−4161

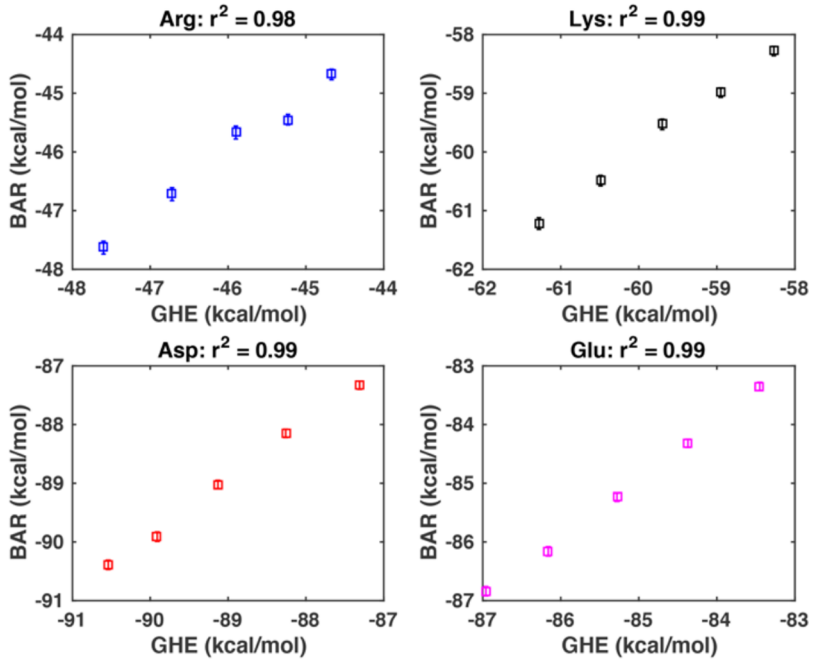

Figure 4. Assessment of the correlation between temperature-dependent intrinsic free energies of hydration calculated using the integral of the Gibbs−Helmholtz equation (GHE) and direct calculations from AMOEBA-based simulations.

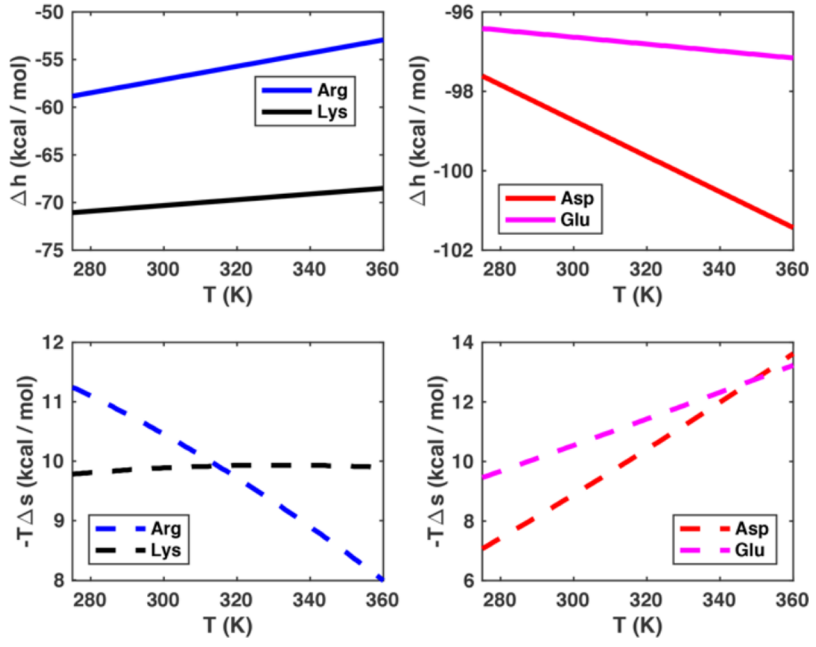

Figure 5. Temperature-dependent enthalpies and entropies of hydration for the four model compound mimics of Arg^+, Lys^+, Asp^-, and Glu^-. These decompositions were calculated using the integral of the Gibbs−Helmholtz equation and parameters from Table 5.

Table 6. Parameters for Δh and Δc_p Extracted from a Nonlinear Least Squares Analysis of Computed Temperature-Dependent Free Energies and Fits to eq 3

solute	$\Delta\mu_h$ at 298 K	estimated Δh at 298 K (kcal/mol)	estimated Δc_p (cal/(mol K))
Cl^-	−86.17 ± 0.06	−87.72	−46.55
Cl^0	2.50 ± 0.04	−2.70	63.31
Cl^+	−65.30 ± 0.05	−68.65	11.35

systems, water molecules within the first hydration shell around each solute were used to compute the $\rho(r,\theta)$ distributions. For each system, $\rho(r,\theta)\delta r\delta\theta$ quantifies the probability that a pair of water molecules will be in a distance interval r and $r + \theta r$ *and* have relative orientations that are between θ and $\theta + \delta\theta$.

Optimal hydrogen bonding is realized for short distances and values of θ that are close to zero. These results are shown in Figure 8. The basin corresponding to $r \approx 2.8$ Å and values of $\theta <$ 10° are evident in each of the four panels of Figure 8, and these peaks represent the optimal hydrogen-bonded geometries for water molecules. This peak becomes pronounced for Cl^0 and Cl^+, which are the alchemic neutral and cationic solutes, respectively. The density in the interval $3 < r$, Å < 7 and $0° < \theta <$

https://doi.org/10.1021/acs.jpcb.1c01073
J. Phys. Chem. B 2021, 125, 4148−4161

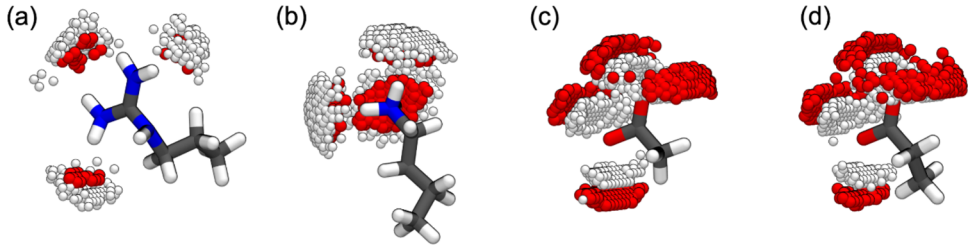

Figure 6. Hydration structures around the model compounds mimicking the side chains of (a) Arg^+, (b) Lys^+, (c) Asp^- and (d) Glu^-. The red and white spheres around the model compounds denote areas with a time-averaged density of water oxygen and hydrogen atoms being larger than 0.2 $Å^{-3}$. Positions further than 2 Å away from the model compound are not shown. To calculate the density, we define two vectors $\vec{r}_y$ and $\vec{r}_{xy}$ for the model compounds to align all the frames in the trajectory. All the coordinates for atoms in the frame are translated and rotated so that the central atom in the model compound is in the origin of the simulation box and $\vec{r}_y$ points to the y direction and $\vec{r}_{xy}$ is in the x-y plane. For (a), the central atom is the carbon atom in the guanidine group, $\vec{r}_y$ is the vector pointing from the central atom to the nitrogen atom bonded with two carbon atoms, and $\vec{r}_{xy}$ is the vector pointing from the central atom to one of the nitrogen atoms bonded with two hydrogens. For (b), the central atom is the nitrogen atom, $\vec{r}_y$ is the vector pointing from the central atom to the carbon atom bonded with nitrogen, and $\vec{r}_{xy}$ is the vector pointing from the central atom to one of the three hydrogens bonded with it. (c, d) The central atom is the carbon atom bonded with oxygen atoms, $\vec{r}_y$ is the vector pointing from the central atom to the carbon atoms bonded with the central atom, and $\vec{r}_{xy}$ is the vector pointing from the central atom to one of the oxygen atoms. Each panel was made using VMD.[73]

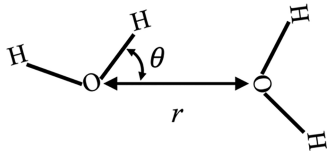

Figure 7. Definition of r and θ for characterizing water structures as defined by Gallagher and Sharp.[75] Here, r is the distance between two water oxygen atoms, and θ is the smallest angle in the four $O{-}O_x{-}H_x$ angles, where H_x is bonded with O_x.

60° is significantly higher for water in the presence of the anion when compared to neat water or in the presence of the uncharged, nonpolar Cl^0 solute. In this region, there are two distinct peaks, and this increased density is consistent with the calculated negative Δc_P values in that it points to distinct structural preferences of water molecules in the presence of anionic solutes. In contrast, for water around the cationic Cl^+ solute, the density is dispersed across the interval $3 < r, Å < 7$ and $40° < \theta < 120°$, that is, reflected about an axis that intersects the ordinate at ∼40°. As with the uncharged Cl^0 solute, there is a sharp density for water in the regime corresponding to optimal hydrogen bonding, and this is weakened as r increases for the Cl^+ solute.

Figure 9 shows difference density distributions $\Delta\rho(r,\theta)$, where for each solute X, the difference distribution is calculated as $\rho_X(r,\theta) - \rho_w(r,\theta)$, where $\rho_X(r,\theta)$ and $\rho_w(r,\theta)$ are the joint distributions for the solute−solvent system with solute X and

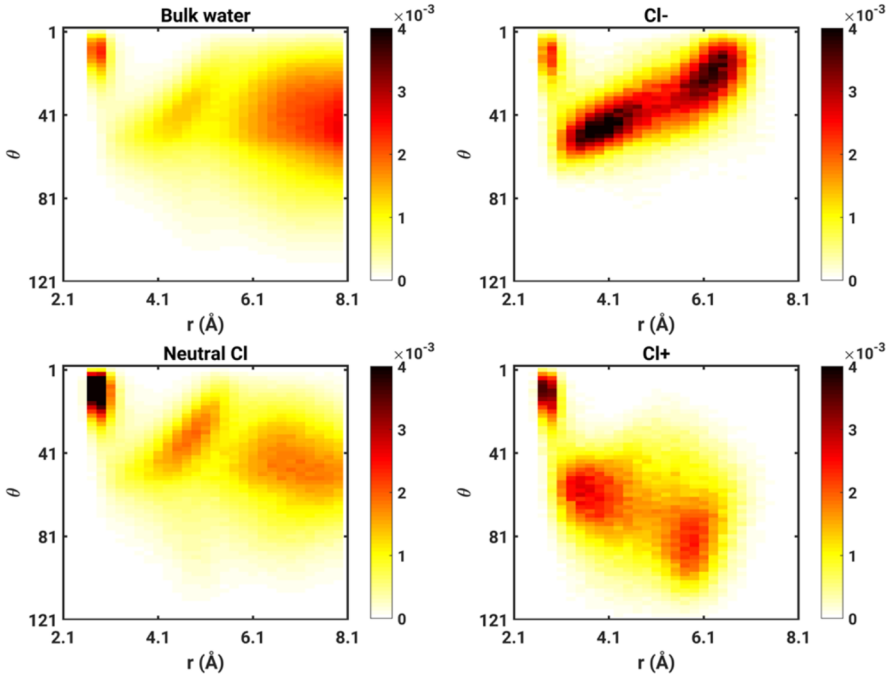

Figure 8. Joint distributions r and θ (see Figure 6) for bulk water and the waters in the first solvation shell of Cl^-, Cl^0 (neutral Cl), and Cl^+ at 298 K. For Cl^-, Cl^+, and the neutral Cl, the water is considered in the first solvation shell if the distance from the solute to the water oxygen atom is smaller than the radius of the first solvation shell, which is 4.0, 3.9, and 5.4 Å for Cl^-, Cl^+, and neutral Cl, respectively. For each system, the histogram is calculated from a 6 ns long trajectory with a saving interval of 1 ps. The bin size is 0.2 Å for r and 2° for θ.

https://doi.org/10.1021/acs.jpcb.1c01073
J. Phys. Chem. B 2021, 125, 4148−4161

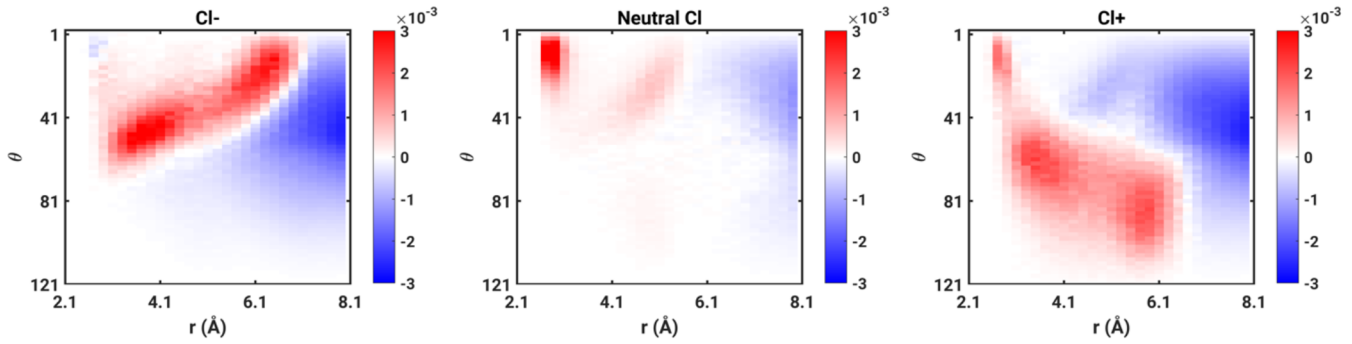

Figure 9. Difference density distributions for the three reference systems.

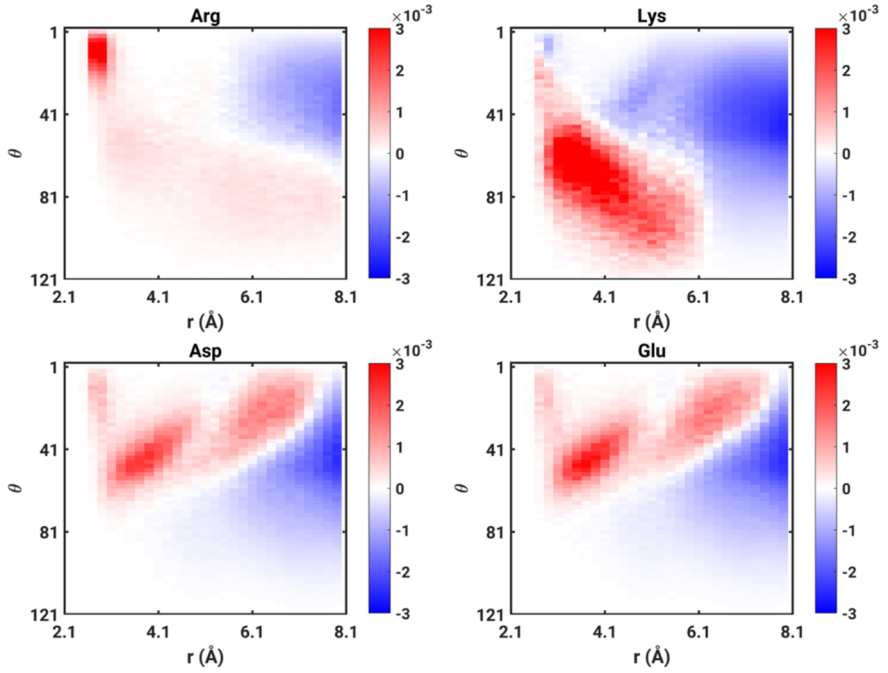

Figure 10. Difference density distributions for the model compounds mimicking the side chains of the charged amino acids referenced to that of neat water. The comparisons are shown for 298 K.

neat water, respectively. In these difference distribution plots, regions where there is an enhancement of density vis-à-vis neat water are in hot colors, whereas the regions where there is a depletion of density compared to neat water are shown in cool colors. The difference distributions highlight the fundamental differences between hydrophobic hydration seen for Cl^0 and the anion versus cation systems.

Next, we analyzed the difference density distributions for model compounds that mimic Arg^+, Lys^+, Asp^-, and Glu^-, respectively. The results, shown in Figure 10, show that the difference density distributions for Arg^+ and Lys^+ are clearly very different from one another. When compared to neat water, there is a significant increase of density in the basin corresponding to $r \approx 2.8$ Å and $\theta < 10°$ for Arg^+. This increase is similar to that of the model hydrophobic solute Cl^0. For Lys^+, the density in the basin corresponding to $r \approx 2.8$ Å and values of $\theta < 10°$ is considerably lower than that of neat water or the model hydrophobic solute Cl^0. Instead, there is a pronounced increase in density in the region corresponding to $3 < r$, Å < 7 and $40° < \theta < 120°$, which is concordant with the observations for Cl^+, although the distribution is considerably more uniform for Lys^+. The difference density distributions for Asp^- and Glu^- are qualitatively similar to that observed for Cl^-, showing increased preference for the interval $3 < r$, Å < 7 and $0° < \theta < 60°$ and a clear weakening, vis-à-vis neat water, for the basin corresponding to $r \approx 2.8$ Å and values of $\theta < 10°$. Taken together, these features indicate that Arg^+ behaves more like a hydrophobic solute when compared and Lys^+, and the impact of the anionic moieties on the water structure is mutually consistent, being qualitatively similar to that of Cl^- while also providing a rationalization for the negative heat capacities reported for these solutes.

Finally, we computed the numbers of water molecules that make up the first hydration shells around each of the four solutes. On average, there are 15 water molecules in the first shell around Arg^+, ~9 water molecules in the first shell around Asp^- and Glu^-, and ~5 water molecules in the first shell around Lys^+. The larger numbers of water molecules around Arg are concordant with signatures of hydrophobic hydration when compared to Lys^+, Asp^-, or Glu^-. On the basis of the estimates for the average numbers of water molecules in the first hydration shells, it follows that the free energy of hydration per water molecule is ca. −3 kcal/mol for Arg^+, ca. −12 kcal/mol for Lys^+,

https://doi.org/10.1021/acs.jpcb.1c01073
J. Phys. Chem. B 2021, 125, 4148−4161

Table A1. Intrinsic Free Energies of Hydration of 1-Butylammonium Obtained at Different Temperatures Calculated using BAR and MBAR Methods[a]

	275 K	298 K	323 K	348 K	373 K
BAR	−61.22 ± 0.10	−60.49 ± 0.09	−59.53 ± 0.09	−58.99 ± 0.08	−58.28 ± 0.08
MBAR[b]	−61.23 ± 0.05	−60.50 ± 0.05	−59.53 ± 0.06	−58.98 ± 0.05	−58.25 ± 0.06

[a]The lambda interval is 0.10, and the corresponding lambda schedule is listed in Table A2. [b]To increase the computational efficiency of MBAR calculations, the lambda schedule was divided into four parts: {(0.0, 0.0), (0.0, 0.1), (0.0, 0.2), (0.0, 0.3), (0.0, 0.4), (0.0, 0.5)}, {(0.0, 0.5), {(0.0, 0.6), (0.0, 0.7), (0.0, 0.8), (0.0, 0.9), (0.0, 1.0)}, {(0.0, 1.0), (0.1, 1.0), (0.2, 1.0), (0.3, 1.0), (0.4, 1.0), (0.5, 1.0)} and {(0.5, 1.0), (0.6, 1.0), (0.7, 1.0), (0.8, 1.0), (0.9, 1.0), (1.0, 1.0)}. For each of these four parts, one independent MBAR calculation was performed to obtain the free energy difference between two neighboring windows.

ca. −10 kcal/mol for Asp^+, and ca. −9.6 kcal/mol for Glu^-. These estimates suggest that the free energy cost for displacing individual water molecules from the first hydration shell will be smallest for Arg^+, largest for Lys^+, and ∼10 kcal/mol per molecule for Asp^-/Glu^-.

4. DISCUSSION

4.1. Summary of Main Findings. We introduced our adaptation of the TCPD approach to estimate free energies of hydration from direct measurements of accessible quantities. The measured values are taken from the literature. Unfortunately, the persistent and large uncertainties associated with the free energy of hydration of the proton prevent us from obtaining precise values for $\Delta\mu_h$ of Arg^+, Lys^+, Asp^-, and Glu^-. However, the TCPD formalism allows one to estimate the relevant free energies of hydration that would be consistent with force field specific values for $\Delta\mu_h^{H^+}$. By collating 72 distinct values for $\Delta\mu_h^{H^+}$ from the literature (Table 1), we were able to estimate mean values of the free energies of hydration for Arg^+, Lys^+, Asp^-, and Glu^- (Table 2). Overall, the TCPD-based estimations point to clear trends regarding the free energies of hydration, and these are corroborated by direct calculations of intrinsic and corrected values obtained using the AMOEBA force field.

Using intrinsic free energies of hydration that were calculated at different temperatures, we obtained estimates for the enthalpy of hydration at a reference temperature of 298 K and the heat capacity of hydration. The latter was estimated by assuming that the heat capacity of hydration is independent of temperature. This is a reasonable assumption, and its validity is assessed by the quality of the agreement between the direct calculations of $\Delta\mu_h$ as a function of temperature and the values we obtain using the integral of the Gibbs−Helmholtz equation.

Overall, we report three main results: (1) Arg^+ and Lys^+ are nonequivalent in terms of their hydration preferences. Contrary to expectations based on partition coefficients between water and octanol,[78] the hydration free energy we obtain for Arg^+ is consistently less favorable than that of Lys^-. Additionally, the heat capacity of hydration, which is positive for both species, is ∼2.3 times larger for Arg^+ when compared to Lys^+. This large heat capacity of hydration is indicative of a more hydrophobic character for Arg. (2) The free energies of hydration for acidic residues are considerably more favorable than for basic residues. (3) The heat capacity of hydration is negative for Asp^- and Glu^-. Negative heat capacities have been attributed to differences in hydration structure and the propagation of these effects beyond the first hydration shell. This is evident in the difference density distributions that we compute for the negatively charged solutes.

Measurements have reported negative heat capacities of hydration for whole salts, and this has been taken to imply that hydrophilic hydration, that is, the hydration of anions as well as cations, is associated with negative values for Δc_p.[79] This inference has been questioned by Sedlmeier and Netz.[77] They showed that, while the sum of heat capacities for anions and cations in whole salts can be negative, the negative Δc_p values arise strictly from the anions. Their work uses the SPC/E water model and nonpolarizable force fields. Accordingly, it appears that the negative heat capacity of hydration for anions is a generic and robust attribute that does not depend on polarizability. Indeed, we find that the negative heat capacity is evident for Cl^- ions, whereas the heat capacity is positive for alchemically transformed Cl^+ and Cl^0 solutes.

4.2. Relevance of Our Findings to Recent Studies on IDPs. Ongoing investigations of the determinants of driving forces of phase separation in IDPs and in RNA binding domains have revealed striking differences in the contributions of charged side chains to the driving forces for phase separation.[80] The most salient observation is that Arg and Lys are fundamentally different[81] as drivers of phase separation.[80,82] Replacing Arg residues with Lys significantly weakens the driving forces for phase separation in a variety of systems.[83] In a similar vein, Sørensen and Kjaergaard recently showed that Arg-rich polyampholytic IDPs prefer considerably more compact conformations when compared to Lys-rich counterparts.[84]

Various conjectures have been offered to explain the differences between Arg^+ and Lys^+ as drivers of phase separation and their differences on conformational equilibria of IDPs. The "Y-aromaticity" of Arg^+, its high quadrupole moment, favorable interactions with π-systems, and the apparent ability to engage in water-mediated attractive interactions have been implicated as features that distinguish Arg^+ from Lys^+ residues as more potent drivers of phase separation.[2,83] However, a definitive rationale for explaining the differences between Arg and Lys and the manifest differences between the contributions of Asp/Glu versus Arg/Lys has been lacking. Our results suggest that differences in free energies of hydration and hydration structure are likely explanations for the intrinsic differences in charged side chains as determinants of conformational and phase equilibria of IDPs—a hypothesis that is being tested in ongoing work.

■ APPENDIX A

We assessed the statistical robustness of our of intrinsic free energies ($\Delta\mu_{h,intrinsic}$) by querying the sensitivity of our results obtained using BAR versus MBAR. We also assessed the impact of the lambda schedule on the estimates of estimates of $\Delta\mu_{h,intrinsic}$. Table A1 shows comparative assessments of the temperature dependent values for $\Delta\mu_{h,intrinsic}$ obtained using BAR versus MBAR.

As summarized in Table A1, the values we obtain for the intrinsic free energies of 1-butylammonium are essentially identical obtained using BAR versus MBAR. This consistency prevails irrespective of the simulation temperature. Next, we

https://doi.org/10.1021/acs.jpcb.1c01073
J. Phys. Chem. B 2021, 125, 4148−4161

Table A2. Lambda Schedules Associated with Distinct Lambda Intervals

lambda interval	lambda schedule for $(\lambda_{ele},\lambda_{vdw})$
0.05	{(0.0, 0.0), (0.0, 0.05), (0.0, 0.1), (0.0, 0.15), (0.0, 0.2), (0.0, 0.25),(0.0, 0.3), (0.0, 0.35), (0.0, 0.4), (0.0, 0.45), (0.0, 0.5), (0.0, 0.55),(0.0, 0.6), (0.0, 0.65), (0.0, 0.7), (0.0, 0.75), (0.0, 0.8), (0.0, 0.85),(0.0, 0.9), (0.0, 0.95), (0.0, 1.0), (0.05, 1.0), (0.1, 1.0), (0.15, 1.0),(0.2, 1.0), (0.25, 1.0), (0.3, 1.0), (0.35, 1.0), (0.4, 1.0), (0.45, 1.0),(0.5, 1.0), (0.55, 1.0), (0.6, 1.0), (0.65, 1.0), (0.7, 1.0), (0.75, 1.0),(0.8, 1.0), (0.85, 1.0), (0.9, 1.0), (0.95, 1.0), (1.0, 1.0)}
0.10	{(0.0, 0.0), (0.0, 0.1), (0.0, 0.2), (0.0, 0.3), (0.0, 0.4), (0.0, 0.5),(0.0, 0.6), (0.0, 0.7), (0.0, 0.8), (0.0, 0.9), (0.0, 1.0), (0.1, 1.0),(0.2, 1.0), (0.3, 1.0), (0.4, 1.0), (0.5, 1.0), (0.6, 1.0), (0.7, 1.0),(0.8, 1.0), (0.9, 1.0), (1.0, 1.0)}
0.15	{(0.0, 0.0), (0.0, 0.15), (0.0, 0.3), (0.0, 0.45), (0.0, 0.6), (0.0, 0.75),(0.0, 0.9), (0.0, 1.0), (0.15, 1.0), (0.3, 1.0), (0.45, 1.0), (0.6, 1.0),(0.75, 1.0), (0.9, 1.0), (1.0, 1.0)}
0.20	{(0.0, 0.0), (0.0, 0.2), (0.0, 0.4), (0.0, 0.6), (0.0, 0.8), (0.0, 1.0),(0.2, 1.0), (0.4, 1.0), (0.6, 1.0), (0.8, 1.0), (1.0, 1.0)}
0.25	{(0.0, 0.0), (0.0, 0.25), (0.0, 0.5), (0.0, 0.75), (0.0, 1.0),(0.25, 1.0), (0.5, 1.0), (0.75, 1.0), (1.0, 1.0)}

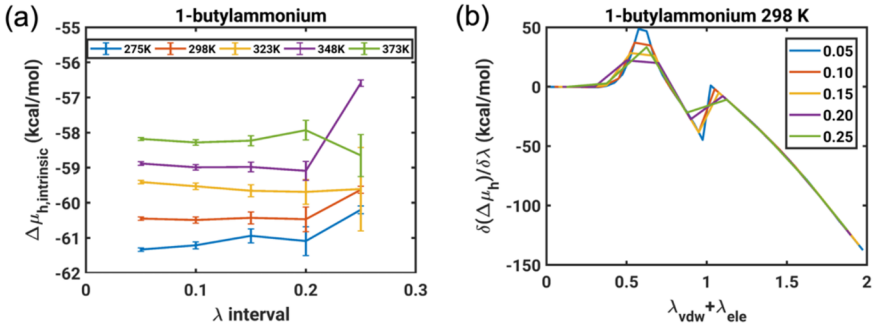

Figure A1. Assessment of the statistical robustness of free energy calculations based on the AMOEBA force field. (a) Intrinsic free energy of hydration ($\Delta\mu_{h,intrinsic}$) for 1-butylammonium at different temperatures calculated using the BAR method with different lambda intervals. The corresponding lambda schedules are listed in Table A2. (b) Plots of the derivative $\delta(\Delta\mu_h)/\delta\lambda$ for 1-butylammonium calculated using different lambda intervals using data obtained at 298 K.

assessed the impact of the lambda schedule on the free energy estimates obtained using BAR. The different lambda schedules used are tabulated in Table A2.

The results we obtain for different lambda schedules are summarized in Figure A1. Notice that the estimates we obtain deviate significantly from one another only when the lambda schedule is too coarse, that is, for the lambda interval of 0.25. For more realistic and numerically conservative lambda schedules, the estimates we obtain are robust and insensitive to the details of the lambda schedule.

AUTHOR INFORMATION

Corresponding Author

Rohit V. Pappu − *Department of Biomedical Engineering and Center for Science & Engineering of Living Systems, Washington University in St. Louis, St. Louis, Missouri 63130, United States;* orcid.org/0000-0003-2568-1378; Email: pappu@wustl.edu

Authors

Martin J. Fossat − *Department of Biomedical Engineering and Center for Science & Engineering of Living Systems, Washington University in St. Louis, St. Louis, Missouri 63130, United States*

Xiangze Zeng − *Department of Biomedical Engineering and Center for Science & Engineering of Living Systems, Washington University in St. Louis, St. Louis, Missouri 63130, United States;* orcid.org/0000-0002-9848-3033

Complete contact information is available at: https://pubs.acs.org/10.1021/acs.jpcb.1c01073

Author Contributions

†(M.J.F. and X.Z.) Co-first authors.

Notes

The authors declare no competing financial interest.

ACKNOWLEDGMENTS

We thank the anonymous reviewer for the constructive criticisms and helpful suggestions. We are grateful for the privilege of contributing this work as part of the festschrift celebrating Professor Dev Thirumalai's numerous and influential contributions to physical chemistry, soft matter physics, and biophysics. Professor Thirumalai has been an inspiration and a generous mentor over the years. We are grateful to C. Liu and P. Ren for their collaboration on the original free-energy calculations,[4] developing parameters for the AMOEBA force field, and technical assistance. Our work is supported by grants from the U.S. National Science Foundation (DMR1729783) and the U.S. National Institutes of Health (5R01NS056114).

REFERENCES

(1) Das, R. K.; Ruff, K. M.; Pappu, R. V. Relating sequence encoded information to form and function of intrinsically disordered proteins. *Curr. Opin. Struct. Biol.* **2015**, *32*, 102−12.

(2) Wang, J.; Choi, J.-M.; Holehouse, A. S.; Zhang, X.; Jahnel, M.; Lemaitre, R.; Maharana, S.; Pozniakovsky, A.; Drechsel, D.; Poser, I.; Pappu, R. V.; Alberti, S.; Hyman, A. A.; et al. A molecular grammar underlying the driving forces for phase separation of prion-like RNA binding proteins. *Cell* **2018**, *174*, 688−699.

(3) Auton, M.; Bolen, D. W. Additive Transfer Free Energies of the Peptide Backbone Unit That Are Independent of the Model Compound and the Choice of Concentration Scale. *Biochemistry* **2004**, *43* (5), 1329−1342.

(4) Zeng, X.; Liu, C.; Fossat, M. J.; Ren, P.; Chilkoti, A.; Pappu, R. V. Design of intrinsically disordered proteins that undergo phase transitions with lower critical solution temperatures. *APL Mater.* **2021**, *9*, 021119.

(5) Thirumalai, D.; Samanta, H. S.; Maity, H.; Reddy, G. Universal Nature of Collapsibility in the Context of Protein Folding and Evolution. *Trends Biochem. Sci.* **2019**, *44* (8), 675−687.
(6) O'Brien, E. P.; Ziv, G.; Haran, G.; Brooks, B. R.; Thirumalai, D. Effects of denaturants and osmolytes on proteins are accurately predicted by the molecular transfer model. *Proc. Natl. Acad. Sci. U. S. A.* **2008**, *105* (36), 13403.
(7) Ben-Naim, A.; Ting, K.-L.; Jernigan, R. L. Solvation thermodynamics of biopolymers. I. Separation of the volume and surface interactions with estimates for proteins. *Biopolymers* **1989**, *28* (7), 1309−1325.
(8) Wolfenden, R. Interaction of the peptide bond with solvent water: a vapor phase analysis. *Biochemistry* **1978**, *17* (1), 201−204.
(9) (a) Makhatadze, G. I.; Lopez, M. M.; Privalov, P. L. Heat capacities of protein functional groups. *Biophys. Chem.* **1997**, *64* (1), 93−101. (b) Makhatadze, G. I.; Privalov, P. L. Contribution of Hydration to Protein Folding Thermodynamics: I. The Enthalpy of Hydration. *J. Mol. Biol.* **1993**, *232* (2), 639−659.
(10) (a) Marcus, Y. The hydration entropies of ions and their effects on the structure of water. *J. Chem. Soc., Faraday Trans. 1* **1986**, *82* (1), 233−242. (b) Marcus, Y. Electrostriction, Ion Solvation, and Solvent Release on Ion Pairing. *J. Phys. Chem. B* **2005**, *109* (39), 18541−18549.
(11) Grossfield, A.; Ren, P.; Ponder, J. W. Ion Solvation Thermodynamics from Simulation with a Polarizable Force Field. *J. Am. Chem. Soc.* **2003**, *125* (50), 15671−15682.
(12) Marcus, Y.; Hefter, G. Ion Pairing. *Chem. Rev.* **2006**, *106* (11), 4585−4621.
(13) Pearson, R. G. Ionization potentials and electron affinities in aqueous solution. *J. Am. Chem. Soc.* **1986**, *108* (20), 6109−6114.
(14) Fitch, C. A.; Platzer, G.; Okon, M.; Garcia-Moreno E, B.; McIntosh, L. P. Arginine: Its pKa value revisited. *Protein Sci.* **2015**, *24* (5), 752−761.
(15) Sitkoff, D.; Sharp, K. A.; Honig, B. Accurate Calculation of Hydration Free Energies Using Macroscopic Solvent Models. *J. Phys. Chem.* **1994**, *98* (7), 1978−1988.
(16) Pliego, J. R.; Riveros, J. M. New values for the absolute solvation free energy of univalent ions in aqueous solution. *Chem. Phys. Lett.* **2000**, *332* (5), 597−602.
(17) Zhang, H.; Jiang, Y.; Yan, H.; Yin, C.; Tan, T.; van der Spoel, D. Free-Energy Calculations of Ionic Hydration Consistent with the Experimental Hydration Free Energy of the Proton. *J. Phys. Chem. Lett.* **2017**, *8* (12), 2705−2712.
(18) Tissandier, M. D.; Cowen, K. A.; Feng, W. Y.; Gundlach, E.; Cohen, M. H.; Earhart, A. D.; Tuttle, T. R.; Coe, J. V. The Proton's Absolute Aqueous Enthalpy and Gibbs Free Energy of Solvation from Cluster Ion Solvation Data. *J. Phys. Chem. A* **1998**, *102* (46), 9308−9308.
(19) Hunter, E. P. L.; Lias, S. G. Evaluated Gas Phase Basicities and Proton Affinities of Molecules: An Update. *J. Phys. Chem. Ref. Data* **1998**, *27* (3), 413−656.
(20) Bodnarchuk, M. S.; Heyes, D. M.; Dini, D.; Chahine, S.; Edwards, S. Role of Deprotonation Free Energies in pKa Prediction and Molecule Ranking. *J. Chem. Theory Comput.* **2014**, *10* (6), 2537−2545.
(21) Jorgensen, W. L.; Briggs, J. M. A priori pKa calculations and the hydration of organic anions. *J. Am. Chem. Soc.* **1989**, *111* (12), 4190−4197.
(22) Stull, D. R. Vapor Pressure of Pure Substances. Organic and Inorganic Compounds. *Ind. Eng. Chem.* **1947**, *39* (4), 517−540.
(23) Stover, M. L.; Jackson, V. E.; Matus, M. H.; Adams, M. A.; Cassady, C. J.; Dixon, D. A. Fundamental Thermochemical Properties of Amino Acids: Gas-Phase and Aqueous Acidities and Gas-Phase Heats of Formation. *J. Phys. Chem. B* **2012**, *116* (9), 2905−2916.
(24) Lee, S.; Cho, K.-H.; Lee, C. J.; Kim, G. E.; Na, C. H.; In, Y.; No, K. T. Calculation of the Solvation Free Energy of Neutral and Ionic Molecules in Diverse Solvents. *J. Chem. Inf. Model.* **2011**, *51* (1), 105−114.
(25) Lamoureux, G.; Roux, B. Absolute Hydration Free Energy Scale for Alkali and Halide Ions Established from Simulations with a Polarizable Force Field. *J. Phys. Chem. B* **2006**, *110* (7), 3308−3322.
(26) Schmid, R.; Miah, A. M.; Sapunov, V. N. A new table of the thermodynamic quantities of ionic hydration: values and some applications (enthalpy-entropy compensation and Born radii). *Phys. Chem. Chem. Phys.* **2000**, *2* (1), 97−102.
(27) Krestov, G. A. *Thermodynamics of Solvation, Solution and Dissolution; Ions and Solvents; Structure and Energetics;* Ellis Horwood Ltd.: New York, NY, 1991.
(28) Marković, Z.; Tošović, J.; Milenković, D.; Marković, S. Revisiting the solvation enthalpies and free energies of the proton and electron in various solvents. *Comput. Theor. Chem.* **2016**, *1077*, 11−17.
(29) Asthagiri, D.; Pratt, L. R.; Ashbaugh, H. S. Absolute hydration free energies of ions, ion-water clusters, and quasichemical theory. *J. Chem. Phys.* **2003**, *119* (5), 2702−2708.
(30) Latimer, W. M.; Pitzer, K. S.; Slansky, C. M. The Free Energy of Hydration of Gaseous Ions, and the Absolute Potential of the Normal Calomel Electrode. *J. Chem. Phys.* **1939**, *7* (2), 108−111.
(31) Carvalho, N. F.; Pliego, J. R. Cluster-continuum quasichemical theory calculation of the lithium ion solvation in water, acetonitrile and dimethyl sulfoxide: an absolute single-ion solvation free energy scale. *Phys. Chem. Chem. Phys.* **2015**, *17* (40), 26745−26755.
(32) Marcus, Y. Thermodynamics of solvation of ions. Part 5.—Gibbs free energy of hydration at 298.15 K. *J. Chem. Soc., Faraday Trans.* **1991**, *87* (18), 2995−2999.
(33) Duignan, T. T.; Baer, M. D.; Schenter, G. K.; Mundy, C. J. Real single ion solvation free energies with quantum mechanical simulation. *Chemical Science* **2017**, *8* (9), 6131−6140.
(34) Vlcek, L.; Chialvo, A. A.; Simonson, J. M. Correspondence between Cluster-Ion and Bulk Solution Thermodynamic Properties: On the Validity of the Cluster-Pair-Based Approximation. *J. Phys. Chem. A* **2013**, *117* (44), 11328−11338.
(35) Friedman, H. L.; Krishnan, C. V. Thermodynamics of Ionic Hydration. In *Aqueous Solutions of Simple Electrolytes;* Franks, F., Ed.; Springer US: Boston, MA, 1973; pp 1−118.
(36) Fawcett, W. R. The Ionic Work Function and its Role in Estimating Absolute Electrode Potentials. *Langmuir* **2008**, *24* (17), 9868−9875.
(37) Yu, H.; Whitfield, T. W.; Harder, E.; Lamoureux, G.; Vorobyov, I.; Anisimov, V. M.; MacKerell, A. D.; Roux, B. Simulating Monovalent and Divalent Ions in Aqueous Solution Using a Drude Polarizable Force Field. *J. Chem. Theory Comput.* **2010**, *6* (3), 774−786.
(38) Zhan, C.-G.; Dixon, D. A. Absolute Hydration Free Energy of the Proton from First-Principles Electronic Structure Calculations. *J. Phys. Chem. A* **2001**, *105* (51), 11534−11540.
(39) Hofer, T. S.; Hünenberger, P. H. Absolute proton hydration free energy, surface potential of water, and redox potential of the hydrogen electrode from first principles: QM/MM MD free-energy simulations of sodium and potassium hydration. *J. Chem. Phys.* **2018**, *148* (22), 222814.
(40) Tawa, G. J.; Topol, I. A.; Burt, S. K.; Caldwell, R. A.; Rashin, A. A. Calculation of the aqueous solvation free energy of the proton. *J. Chem. Phys.* **1998**, *109* (12), 4852−4863.
(41) Prasetyo, N.; Hünenberger, P. H.; Hofer, T. S. Single-ion thermodynamics from first principles: Calculation of the absolute hydration free energy and single-electrode potential of aqueous Li+ using ab initio quantum mechanical/molecular mechanical molecular dynamics simulations. *J. Chem. Theory Comput.* **2018**, *14* (12), 6443−6459.
(42) Reif, M. M.; Hünenberger, P. H. Computation of methodology-independent single-ion solvation properties from molecular simulations. IV. Optimized Lennard-Jones interaction parameter sets for the alkali and halide ions in water. *J. Chem. Phys.* **2011**, *134* (14), 144104.
(43) Tuttle, T. R.; Malaxos, S.; Coe, J. V. A New Cluster Pair Method of Determining Absolute Single Ion Solvation Energies Demonstrated in Water and Applied to Ammonia. *J. Phys. Chem. A* **2002**, *106* (6), 925−932.
(44) Pollard, T. P.; Beck, T. L. The thermodynamics of proton hydration and the electrochemical surface potential of water. *J. Chem. Phys.* **2014**, *141* (18), 18C512.

https://doi.org/10.1021/acs.jpcb.1c01073
J. Phys. Chem. B 2021, 125, 4148−4161

(45) Matsui, T.; Kitagawa, Y.; Okumura, M.; Shigeta, Y.; Sakaki, S. Consistent scheme for computing standard hydrogen electrode and redox potentials. *J. Comput. Chem.* **2013**, *34* (1), 21−26.
(46) Kelly, C. P.; Cramer, C. J.; Truhlar, D. G. Aqueous Solvation Free Energies of Ions and Ion-Water Clusters Based on an Accurate Value for the Absolute Aqueous Solvation Free Energy of the Proton. *J. Phys. Chem. B* **2006**, *110* (32), 16066−16081.
(47) (a) Rossini, E.; Knapp, E.-W. Proton solvation in protic and aprotic solvents. *J. Comput. Chem.* **2016**, *37* (12), 1082−1091. (b) Rossini, E.; Knapp, E.-W. Erratum: Proton solvation in protic and aprotic solvents. *J. Comput. Chem.* **2016**, *37*, 1082−1091; *J. Comput. Chem.* **2016**, *37* (23), 2163−2164.
(48) Bryantsev, V. S.; Diallo, M. S.; Goddard, W. A., III Calculation of Solvation Free Energies of Charged Solutes Using Mixed Cluster/Continuum Models. *J. Phys. Chem. B* **2008**, *112* (32), 9709−9719.
(49) Ishikawa, A.; Nakai, H. Quantum chemical approach for condensed-phase thermochemistry (III): Accurate evaluation of proton hydration energy and standard hydrogen electrode potential. *Chem. Phys. Lett.* **2016**, *650*, 159−164.
(50) Harger, M.; Li, D.; Wang, Z.; Dalby, K.; Lagardère, L.; Piquemal, J.-P.; Ponder, J.; Ren, P. Tinker-OpenMM: Absolute and relative alchemical free energies using AMOEBA on GPUs. *J. Comput. Chem.* **2017**, *38* (23), 2047−2055.
(51) Tuckerman, M. E.; Berne, B. J.; Martyna, G. J. Molecular dynamics algorithm for multiple time scales: Systems with long range forces. *J. Chem. Phys.* **1991**, *94* (10), 6811−6815.
(52) Bussi, G.; Zykova-Timan, T.; Parrinello, M. Isothermal-isobaric molecular dynamics using stochastic velocity rescaling. *J. Chem. Phys.* **2009**, *130* (7), 074101.
(53) Åqvist, J.; Wennerström, P.; Nervall, M.; Bjelic, S.; Brandsdal, B. O. Molecular dynamics simulations of water and biomolecules with a Monte Carlo constant pressure algorithm. *Chem. Phys. Lett.* **2004**, *384* (4), 288−294.
(54) Darden, T.; York, D.; Pedersen, L. Particle mesh Ewald: An N log(N) method for Ewald sums in large systems. *J. Chem. Phys.* **1993**, *98* (12), 10089−10092.
(55) Essmann, U.; Perera, L.; Berkowitz, M. L.; Darden, T.; Lee, H.; Pedersen, L. G. A smooth particle mesh Ewald method. *J. Chem. Phys.* **1995**, *103* (19), 8577−8593.
(56) Jing, Z.; Liu, C.; Qi, R.; Ren, P. Many-body effect determines the selectivity for Ca2+ and Mg2+ in proteins. *Proc. Natl. Acad. Sci. U. S. A.* **2018**, *115* (32), E7495.
(57) Jiao, D.; Golubkov, P. A.; Darden, T. A.; Ren, P. Calculation of protein-ligand binding free energy by using a polarizable potential. *Proc. Natl. Acad. Sci. U. S. A.* **2008**, *105* (17), 6290.
(58) Bennett, C. H. Efficient estimation of free energy differences from Monte Carlo data. *J. Comput. Phys.* **1976**, *22* (2), 245−268.
(59) Shirts, M. R.; Chodera, J. D. Statistically optimal analysis of samples from multiple equilibrium states. *J. Chem. Phys.* **2008**, *129* (12), 124105.
(60) Harder, E.; Roux, B. On the origin of the electrostatic potential difference at a liquid-vacuum interface. *J. Chem. Phys.* **2008**, *129* (23), 234706.
(61) Simonson, T.; Hummer, G.; Roux, B. Equivalence of M- and P-Summation in Calculations of Ionic Solvation Free Energies. *J. Phys. Chem. A* **2017**, *121* (7), 1525−1530.
(62) Misin, M.; Fedorov, M. V.; Palmer, D. S. Hydration Free Energies of Molecular Ions from Theory and Simulation. *J. Phys. Chem. B* **2016**, *120* (5), 975−983.
(63) Beck, T. L. The influence of water interfacial potentials on ion hydration in bulk water and near interfaces. *Chem. Phys. Lett.* **2013**, *561*−*562*, 1−13.
(64) Moser, A.; Range, K.; York, D. M. Accurate Proton Affinity and Gas-Phase Basicity Values for Molecules Important in Biocatalysis. *J. Phys. Chem. B* **2010**, *114* (43), 13911−13921.
(65) Xu, B.; Jacobs, M. I.; Kostko, O.; Ahmed, M. Guanidinium Group Remains Protonated in a Strongly Basic Arginine Solution. *ChemPhysChem* **2017**, *18* (12), 1503−1506.
(66) Grossfield, A. Dependence of ion hydration on the sign of the ion's charge. *J. Chem. Phys.* **2005**, *122* (2), 024506.
(67) Rosenberg, S. A.; Hueber, A. E.; Aronson, D.; Gouchie, S.; Howard, P. H.; Meylan, W. M.; Tunkel, J. L. Syracuse Research Corporation's Chemical Information Databases. *Science & Technology Libraries* **2003**, *23* (4), 73−87.
(68) Linstrom, P. J.; Mallard, W. G. The NIST Chemistry WebBook: A Chemical Data Resource on the Internet. *J. Chem. Eng. Data* **2001**, *46* (5), 1059−1063.
(69) Tehan, B. G.; Lloyd, E. J.; Wong, M. G.; Pitt, W. R.; Gancia, E.; Manallack, D. T. Estimation of pKa Using Semiempirical Molecular Orbital Methods. Part 2: Application to Amines, Anilines and Various Nitrogen Containing Heterocyclic Compounds. *Quant. Struct.-Act. Relat.* **2002**, *21* (5), 473−485.
(70) Tehan, B. G.; Lloyd, E. J.; Wong, M. G.; Pitt, W. R.; Montana, J. G.; Manallack, D. T.; Gancia, E. Estimation of pKa Using Semiempirical Molecular Orbital Methods. Part 1: Application to Phenols and Carboxylic Acids. *Quant. Struct.-Act. Relat.* **2002**, *21* (5), 457−472.
(71) Shi, Y.; Wu, C.; Ponder, J. W.; Ren, P. Multipole electrostatics in hydration free energy calculations. *J. Comput. Chem.* **2011**, *32* (5), 967−977.
(72) Lin, F.-Y.; Lopes, P. E. M.; Harder, E.; Roux, B.; MacKerell, A. D. Polarizable Force Field for Molecular Ions Based on the Classical Drude Oscillator. *J. Chem. Inf. Model.* **2018**, *58* (5), 993−1004.
(73) Humphrey, W.; Dalke, A.; Schulten, K. VMD: Visual molecular dynamics. *J. Mol. Graphics* **1996**, *14* (1), 33−38.
(74) Prabhu, N. V.; Sharp, K. A. Heat capacity in proteins. *Annu. Rev. Phys. Chem.* **2005**, *56* (1), 521−548.
(75) Gallagher, K. R.; Sharp, K. A. A New Angle on Heat Capacity Changes in Hydrophobic Solvation. *J. Am. Chem. Soc.* **2003**, *125* (32), 9853−9860.
(76) Godawat, R.; Jamadagni, S. N.; Garde, S. Characterizing hydrophobicity of interfaces by using cavity formation, solute binding, and water correlations. *Proc. Natl. Acad. Sci. U. S. A.* **2009**, *106* (36), 15119.
(77) Sedlmeier, F.; Netz, R. R. Solvation thermodynamics and heat capacity of polar and charged solutes in water. *J. Chem. Phys.* **2013**, *138* (11), 115101.
(78) Radzicka, A.; Wolfenden, R. Comparing the polarities of the amino acids: side-chain distribution coefficients between the vapor phase, cyclohexane, 1-octanol, and neutral aqueous solution. *Biochemistry* **1988**, *27* (5), 1664−1670.
(79) Kinoshita, M.; Yoshidome, T. Molecular origin of the negative heat capacity of hydrophilic hydration. *J. Chem. Phys.* **2009**, *130* (14), 144705.
(80) Nott, T. J.; Petsalaki, E.; Farber, P.; Jervis, D.; Fussner, E.; Plochowietz, A.; Craggs, T. D.; Bazett-Jones, D. P.; Pawson, T.; Forman-Kay, J. D.; Baldwin, A. J. Phase transition of a disordered nuage protein generates environmentally responsive membraneless organelles. *Mol. Cell* **2015**, *57* (5), 936−47.
(81) Fisher, R. S.; Elbaum-Garfinkle, S. Tunable multiphase dynamics of arginine and lysine liquid condensates. *Nat. Commun.* **2020**, *11* (1), 4628.
(82) Brady, J. P.; Farber, P. J.; Sekhar, A.; Lin, Y. H.; Huang, R.; Bah, A.; Nott, T. J.; Chan, H. S.; Baldwin, A. J.; Forman-Kay, J. D.; Kay, L. E. Structural and hydrodynamic properties of an intrinsically disordered region of a germ cell-specific protein on phase separation. *Proc. Natl. Acad. Sci. U. S. A.* **2017**, *114* (39), E8194−E8203.
(83) Greig, J. A.; Nguyen, T. A.; Lee, M.; Holehouse, A. S.; Posey, A. E.; Pappu, R. V.; Jedd, G. Arginine-Enriched Mixed-Charge Domains Provide Cohesion for Nuclear Speckle Condensation. *Mol. Cell* **2020**, *77* (6), 1237−1250.
(84) Sørensen, C. S.; Kjaergaard, M. Effective concentrations enforced by intrinsically disordered linkers are governed by polymer physics. *Proc. Natl. Acad. Sci. U. S. A.* **2019**, *116* (46), 23124.

https://doi.org/10.1021/acs.jpcb.1c01073
J. Phys. Chem. B 2021, 125, 4148−4161